Power-Quality Enhancer Using an Artificial Bee Colony-Based Optimal-Controlled Shunt Active-Power Filter

ESSAMUDIN ALI EBRAHIM
Power-Electronics and Energy-Conversion Department
Electronics Research Institute
El-tahrir Street, P. O. Code 12662 Dokki, Cairo,
EGYPT
essamudin@yahoo.com & essamudin@eri.sci.eg

Abstract: - Variable speed drives (VSDs) use power electronic components - as controlled switches - which distort the sinusoidal current and voltage waveforms of AC grid due to harmonic injection at the point of common coupling (PCC). These harmonics and distortions are propagated through the power network and affect all other connected loads. So, the shunt active power filter (SAPF) is one of the proposed tools to mitigate these harmonics. In this paper, an artificial bee colony (ABC)- based optimal-controlled SAPF is proposed to provide instantaneous reactive power compensation required for harmonic mitigation of a separately excited DC motor – as a dynamic load - fed from uncontrolled- bridge rectifier via a GTO-thyristorized-DC chopper. The proposed technique uses three-phase hysteresis-current controller inverter connected with reactors as an active power filter. The dc- link voltage of that inverter is controlled using PID-controller. Tuning of the PID-parameters depends on artificial bee colony optimization. The proposed ABC-controller is employed to search for optimal controller parameters by minimizing the error signal - as an objective function - of a dc-link for the inverter. The performance of the proposed filter that called ABC-SAPF is carried out by simulation under steady-state and dynamic operations using MATLAB/ SIMULINK software. Also, these results are compared with other control approaches as ANN and fuzzy logic. The results show that it is an effective in enhancement dynamic of power quality and also the overall total harmonic distortion (THD) is minimized to safe-limit according to the harmonic restriction standards such as IEEE-519 and IEC 61000.

Key-Words: - Artificial bee colony, power quality, hysteresis current controller, shunt active power filter, Objective function, Scout and Onlookers, point of common coupling, total harmonic distortion.

1 Introduction

Majority of industrial loads are variable speed drives (VSDs) - both ac and dc motors. These drives use power electronic elements –such as diode, SCR, GTO, MOSFET, IGBT, ...etc. - as electronic switches required for speed, current and torque control [1]. DC motor drives require a controlled dc power supply such as uncontrolled bridge rectifiers with dc choppers or thyristor-controller bridge rectifiers [2]. Both techniques cause distortion for supply-voltage and current waveforms. This distortion resulted in a large amount of harmonic injection into distribution system that affects on the other loads on the same point of the common coupling (PCC). Also, these harmonics are responsible for voltage sag and swell, reduction in source power factor (PF), voltage instability, increasing power losses in the network, transformer and other equipments overheating, system malfunctions, electric-equipment damage, feeder overloading, noise interference to adjacent communication systems, shock hazards, operational failure of electronic equipments, …etc [3-5]. These pollution problems lead to more stringent requirements regarding PQ, such as IEEE-519 [6] and IEC 61000-3-2 [7]. Conventionally, passive filters have been used for power quality enhancement. Passive filters have drawbacks such as bulky in size, high no-load losses, no-load over-voltage at the PCC, resonance, un-controlled compensation, …etc [8].

On the other hand, active power filters (APFs) provide effective and dynamic compensation with the help of efficient controllers [9].

APFs are classified to shunt, series and hybrid types. Shunt active power filter (SAPF) has many features such as: low implementation cost, don't create displacement power factor problems and utility loading, supply inductance L_S does not affect the harmonic compensation of parallel active filter system, simple control circuit, can damp harmonic propagation in a distribution feeder or between two distribution feeders, easy to connect in parallel a number of active filter modules in order to achieve

higher power requirements, easy protection and inexpensive isolation switchgear, easy to be installed, and provides immunity from ambient harmonic loads.
In the last two decades, many authors have proposed several techniques for designing SAPF and its control algorithm to enhance the performance and power quality.
There are two classes of the APF control methods: the frequency and time domain. The time domain control method is faster, simple, require minimum memory space and no time consumption through CPU processing and sampling but less accurate comparing to the frequency method. The time domain methods include: the conventional p-q of instantaneous power method, the fundamental frequency d-q method, the synchronous detection method (SDM) and indirect current-control method (ICM) [10-12].
The frequency method depends on the spectral analysis algorithms based on Fast Fourier Transformation (FFT) and Recursive Discrete Fourier Transformation (RDFT) [13,14].
However, both two classes need to estimate reference currents required to generate control signals of pulse width modulation (PWM) inverter.
Several researches suggested intelligent controller such as fuzzy logic, artificial neural network (ANN), or nero-fuzzy logic controller to use it as a controller in estimation loop. In [15], authors proposed ANN adaptive hybrid APF for power quality compensation in induction motor. Also, in [16], authors used ANN in phase-locking scheme for APF to estimate system frequency.
Moreover, in [17], a real-time implementation of hysteresis-band current control technique for SAPF was proposed using adaptive fuzzy logic controller. The proposed controller was used in dc-link voltage regulation instead of classical PI controller. Also, ref. [18] was an improvement of dynamic behavior of SAPF using fuzzy instantaneous power theory. In addition, authors in [19] introduced an ANN –based discrete-fuzzy logic controlled APF for harmonic extraction.
On the other hand, many author used classical proportional integral (PI) and proportional integral derivative (PID) controllers in dc-link for voltage regulation as [14], [20], [21] and [22].
PID controllers have been widely used in industry for many years due to their simplicity of operation, easy to implement and consumes very little time through on-line digital control approach. Unfortunately, robustness and optimization not be achieved with these types of controllers because of high order plants, time delays, parameters uncertainty of plant, and system nonlinearity.
Several efforts to improve PI or PID controllers in voltage regulation were introduced. In [23], the authors suggested a robust adaptive control strategy of active power filters for power-factor correction, harmonic compensation, and balancing of non -linear Loads. The control strategy was adaptive pole-placement. The same authors in [24] proposed a robust dc-link voltage control strategy to enhance the performance of SAPF without harmonic detection schemes. The proposed controller depends on using slide-mode for fine tuning of PI gains. Also, in [25], the authors used Bode diagram with PI and PID controllers for single-phase SAPF.
But, in [26] an active harmonic filter based on one cycle control was proposed.
Recently, the advent of evolutionary computation (EC) such as genetic algorithm (GA), Particle Swarm Optimization (PSO), or germ of intelligent (as ant colony optimization ACO and bacteria foraging BF) techniques have inspired as new techniques for optimal design of PID controllers [27,28].
Then several efforts to optimize PI parameters by using bacteria foraging optimization (BFO) algorithm were introduced as in [29-31].

One such a new algorithm is the Artificial Bee Colony (ABC) algorithm motivated by the intelligent foraging behavior of honey bees.

The ABC algorithm was proposed by Karaboga in 2005 for unconstrained optimization problems [32-37].

So, this paper proposes a new optimization algorithm known as ABC for optimal design of PID-controller used to regulate a dc-link capacitor voltage of the SAPF-inverter. The design problem of the proposed controller is formulated as an optimization problem and ABC is employed to search for optimal controller parameters. This controller is known as ABC-PID controller. This optimized controller is used with SAPF to mitigate harmonics of the supply current due to non-linear dynamic load (DC motor) fed from uncontrolled bridge rectifier through GTO electronic switch. Also, the proposed SAPF uses an efficient and simple control strategy to extract reference currents that compared with actual supply currents in a hysteresis-band current-controlled (PWM) technique. Simulation results of dynamic performance for both SAPF and the motor through starting, transient and steady-state conditions, assure the proposed controller in minimizing THD to its minimum value. Also, most of harmonics are mitigated and the supply power factor (p.f.) is increased to approximately unity. In addition, the performance of that proposed approach is compared with other control strategies such as classical PID, fuzzy-PI, and ANN controllers. However, these

results validate the superiority of the proposed method in tuning process compared with other mentioned controllers.

2 System under study

The proposed system consists of two main parts: power circuit and control part.

2.1 The power circuit

The power circuit is shown in figure 1. It includes: 3-phase ac power supply, SAPF, and non-linear load. SAPF consists of shunt reactor with series resistance, both connected with voltage source IGBT-inverter. The non-linear load is a separately excited dc motor as a dynamic load fed from uncontrolled diode-bridge rectifier through a GTO-dc chopper as a controlled switch.

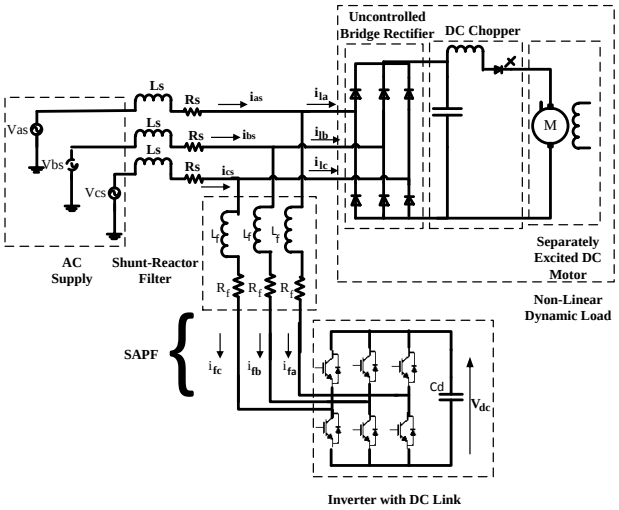

Fig. 1 Power Circuit of SAPF

2.1.1 AC supply model

Under ideal conditions, the three-phase supply voltages are obtained by:

$$\left.\begin{aligned} V_{sa} &= V_m \sin(\omega t) \\ V_{sb} &= V_m \sin(\omega t - 120) \\ V_{sc} &= V_m \sin(\omega t + 120) \end{aligned}\right\} \quad (1)$$

Where, V_m is the peak value of the supply-phase voltage and *ù* is the frequency of the AC source in rad/sec.

The three-phase supply currents can be expressed by:

$$\left.\begin{aligned} i_{sa} &= i_{fa} + i_{la} \\ i_{sb} &= i_{fb} + i_{lb} \\ i_{sc} &= i_{fc} + i_{lc} \end{aligned}\right\} \quad (2)$$

Where $(i_{sa}, i_{sb}$ and $i_{sc})$ are the three-phase supply currents, $(i_{fa}, i_{fb}$ and $i_{fc})$ are the three phase SAPF currents and $(i_{la}, i_{lb}$ and $i_{lc})$ are the three phase load currents.

2.1.2 Mathematical model of dynamic load

The output of three-phase uncontrolled diode bridge rectifier can be given from the following equation:

$$V_o = \frac{3\sqrt{3}\,V_m}{\pi}\left[1 - \sum_{k=1}^{+\infty} \frac{2}{(36K^2-1)} COS\,(6k\omega_o t)\right] \quad (3)$$

Where, $V_m = \sqrt{2} V_{rms}$

V_{rms} = r. m. s phase voltage

So, the output dc component of the bridge is [38,39]:

$$V_o = \frac{3\sqrt{3}\,V_m}{\pi} \approx 1.65 V_m \approx 2.34 V_{rms} \quad (4)$$

On the other hand, the output of the dc chopper is:

$$V_{chopper} = \frac{T_{on}}{T} V_o \,,\; T = T_{on} + T_{off} \quad (5)$$

Where, T_{on} ,T_{off} *and* T are GTO-thyristor on and -off times and periodic duty-cycle time respectively.

Also, the electrical and dynamic equations for separately-excited dc motor can be represented as[40]:

$$v_a(t) = R_a i_a(t) + L_a\left(\frac{d i_a(t)}{dt}\right) + emf(t) \quad (6)$$

$$emf(t) = K_v \omega_a(t) \text{ (constant field current)} \quad (7)$$

$$\omega_a(t) = \frac{d\theta}{dt} \quad (8)$$

$$T_e(t) = J\frac{d\omega(t)}{dt} + B\omega(t) + T_L \quad (9)$$

$$T_e(t) = K_i i_a(t) i_f(t) \quad (10)$$

For constant field current

$$T_e(t) = K_t i_a(t) \quad (11)$$

Where,

$$K_t = K_v K_i \quad (12)$$

$v_a(t), i_a(t)$ *armature input voltage and current*
R_a, L_a *armature resistance and inductance*
emf (t) *induced electromotive force*
$T_e(t), T_L$ *electrical internal and load torques*
$\omega(t), \theta(t)$ *motor angular speed and position*
J *rotor inertia of the motor*
K_b, K_i, K_t *motor constants*

2.1.3 Shunt Active Power Filter (SAPF) model

The active and passive components are combined together to form active filters and these filters need an external source. The passive components are R,L,C and the active component is a voltage source inverter (VSI). The external source is removed and a capacitor is connected on the supply side of the VSI.

The principle of APF is to infuse a current equal in magnitude other than in phase opposition to harmonic current to get a purely sinusoidal current wave in phase with the supply voltage [20],[31].

The controlled currents of the SAPF are given by the following differential equations:

$$\left.\begin{aligned} pi_{fa} &= -(R_f/L_f) i_{fa} + (V_{sa} - V_{fa})/L_f \\ pi_{fb} &= -(R_f/L_f)\, i_{fb} + (V_{sb} - V_{fb})/L_f \\ pi_{fc} &= -(R_f/L_f)\, i_{fc} + (V_{sc} - V_{fc})/L_f \end{aligned}\right\} \quad (13)$$

Where, R_f and L_f are the resistance and the inductance of the SAPF and V_{fa}, V_{fb} and V_{fc} are three-phase SAPF voltages.

The DC capacitor current can be obtained in terms of phase currents (i_{fa}, i_{fb} and i_{fc}) and the switching status of devices (S_a, S_b and S_c).

$$i_{dc} = i_{fa} S_a + i_{fb} S_b + i_{fc} S_c \quad (14)$$

The dc side capacitor voltage can be given by

$$pV_{dc} = (i_{fa} S_a + i_{fb} S_b + i_{fc} S_c)/C_d \quad (15)$$

Where, S_a, S_b and S_C are the switching functions determined by state of the SAPF devices.

The three-phase active power filter voltages can be determined by

$$\left.\begin{aligned} V_{fa} &= (V_{dc}/3)\,(2S_a - S_b - S_c) \\ V_{fb} &= (V_{dc}/3)\,(-S_a + 2S_b - S_c) \\ V_{fc} &= (V_{dc}/3)\,(-S_a - S_b + 2S_c) \end{aligned}\right\} \quad (16)$$

2.2. The control strategy

The block diagram of the proposed control scheme is illustrated in figure 2.

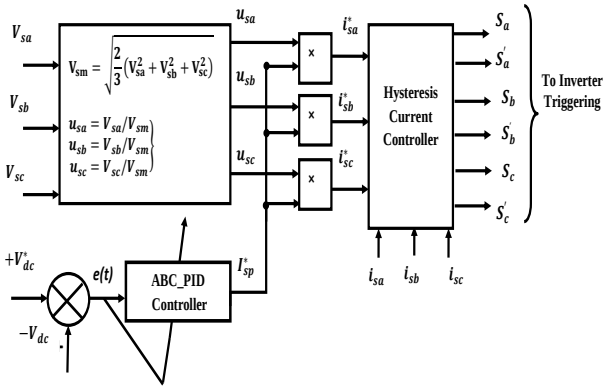

Fig. 2 the block diagram of control scheme

2.2.1 Three-phase reference source currents estimation

Three feedback source-phase voltage signals are sensed and used to compute the rms source phase voltage amplitude V_{sm} as in the following equation:

$$V_{sm} = \sqrt{\frac{2}{3}(V_{sa}^2 + V_{sb}^2 + V_{sc}^2)} \quad (17)$$

Then, unit vector of the source-phase voltages can be computed as:

$$\left.\begin{aligned} u_{sa} &= V_{sa}/V_{sm} \\ u_{sb} &= V_{sb}/V_{sm} \\ u_{sc} &= V_{sc}/V_{sm} \end{aligned}\right\} \quad (18)$$

Now, the reference three-phase source currents (i^*_{sa}, i^*_{sb} and i^*_{sc}) are estimated as:

$$\left.\begin{aligned} i^*_{sa} &= I^*_{sp}\, u_{sa} \\ i^*_{sb} &= I^*_{sp}\, u_{sb} \\ i^*_{sc} &= I^*_{sp}\, u_{sc} \end{aligned}\right\} \quad (19)$$

Where, I^*_{sp} is the peak value of the source current which is the output of the PID controller and will be computed later.

2.2.2 Hysteresis current controller

In this technique, the reference three-phase source currents (i^*_{sa}, i^*_{sb} and i^*_{sc}) are compared with the actual three-phase source currents (i_{sa}, i_{sb} and i_{sc}) to obtain the gating signals to drive IGBT transistor switch of SAPF-inverter. The hysteresis current controller decides the switching pattern of the SAPF inverter according to the pattern:

If $i_{sa} < (i^*_{sa} - HB)$ for leg "a" (S_a=1, $S_a' = 0$), the upper switch of the inverter limb is OFF and the lower switch is ON.

If $i_{sa} > (i^*_{sa} + HB)$ for leg "a" (S_a=0, $S_a' = 1$), the upper switch is ON and the lower switch is OFF.

The switching functions S_b and S_c which are phases leg "b" and leg "c" respectively are formulated similarly by the measured currents (i_{sb} and i_{sc}), the corresponding reference currents (i^*_{sb} and i^*_{sc}) and the hysteresis bandwidth (HB). The hysteresis control principle and the gate pulse can be represented as shown in Fig. 3.

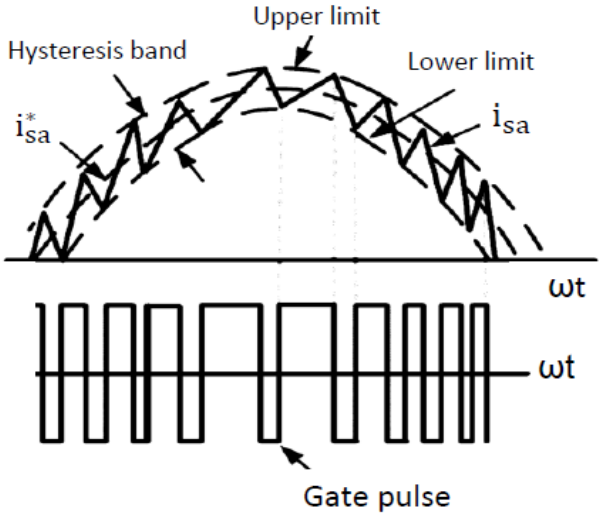

Fig. 3 Hysteresis control principle

3. The proposed ABC-PID controller

For proper compensation, the dc link voltage of the capacitor must be maintained constant to a pre-setting input value as a reference. Then, a suitable and robust controller is required. Many authors suggested classical PID or PI controller as in [14,20-22]. The structure of that classical controller is generally obtained using conventional time/ frequency domain analysis that includes Routh-Hurwitz criterion, pole placement technique, Root

locus method and Ziegler-Nichols tuning formula. Among existing tuning techniques, the Ziegler and Nichols tuning method is mostly used to compute PID gains for the plant. To achieve optimization for controller gains K_p, K_i, K_d, objective function is determined.

The proposed algorithm depends on the foraging behavior of a colony of honey bees in nature. It is called an ABC-PID controller.

All the particles of populations are decoded for K_p, K_i, K_d.

3.1 Formulation of objective function

The controller design is first redrafted as an optimization problem where the objective function comprises time response specifications as steady-state speed error (e_{ss}), which largely depend on controller parameters. Here, the design task is to minimize e_{ss} so this can be performed as an optimization problem by using the following objective function:

$$J = ITAE = \int_0^{\infty} (t^* |e(t)|) dt \quad (20)$$

Where, $e(t) = V_{dc} - V_{dc}^*$ (21)

$V_{dc} = actual\ dc - link\ voltage$

$V_{dc}^* = refernce\ dc - link\ voltage$

$ITAE = Integral\ Time\ Abslute\ Error$

Minimize J:

Subject to the constraint: $\emptyset_{min} \leq \emptyset \leq \emptyset_{max}$

Where $\emptyset$ represents $K_p, K_i, and\ K_d$.

3.2 Artificial Bee Colony (ABC) optimization

ABC as an optimization tool that provides a population based search procedure, in which individuals called food positions are modified by the artificial bees with time and the bees' aim is to discover the places of food sources with high nectar amount and finally the one with highest nectar.

In ABC system, artificial bee fly around in a multi-dimensional search space and some employed and onlooker bees choose food source depending on the experience of themselves and their nest mates, and adjust their positions. Some scouts bees fly and choose the food sources randomly without using experience. If the nectar amount of a new source is higher than that of the previous one in their memory, they memorize the new position and forget the previous one.

In ABC model, the colony consists of three groups of bees: employed, onlookers and scouts. It is assumed that there is only one artificial employed bee for each food source. In other words, the number of employed bees in the colony is equal to the number of food sources around the hive. The employed bees go to their food source and come back to hive and dance on this area. The employed bee whose food source has been abandoned becomes a scout and starts searching a new food source. Onlookers watch the dances of employed bees and choose food sources depending on the dances [32,33].

3.3 Pseudo-codes of the ABC algorithm

1. Load samples of controller parameters
2. Generate the initial population $X_i, i = 1,2,.... FS$
3. Evaluate the fitness (fit_i) of the population
4. Set cycle to 1
5. Repeat
6. For each employed bee {Produce new solution X_{new} by using eqn. (24). Calculate the value (fit_i) by using eqn. (23).Apply greedy selection process}
7. Calculate the probability values (P_i) for the solutions (X_i) by eqn. (22)
8. For each onlooker bee {Select a solution X_i depending on P_i Produce new solution X_{new} Calculate the value fit_i. Apply greedy selection process}
9. If there is an abandoned solution for the scout. Then replace it with a new solution which will be randomly produced by (25)
10. Memorize the best solution so far
11. cycle= cycle+1
12. Until cycle=MCN

Where, X_i represents a solution, fit_i is the fitness value of X_i, X_{new} indicates a neighbor solution of X_i, P_i the probability value of P_i and MCN is the maximum cycle numbers in the algorithm.

3.4 Detailed explanation for the algorithm

In the algorithm, first half of the colony consists of employed artificial bees and the second half constitutes the onlookers. The number of employed bees is equal to the number of food sources (# of solutions in the population).

At first step, the algorithm starts by initializing all employed bees with randomly generated food sources (solutions), where SN denotes the size of population. Each solution $x_i, i = 1,2,.... FS$ is a D-dimensional vector. Where D is the number of optimization parameters. Here, in this study, D- represents the PID-controller parameters to be optimized.

i.e.,$D = [K_p\ K_i\ K_d]$

After initialization, in each iteration of all given cycles, every employed bee finds a food source neighbourhood of its current food source and evaluates its nectar amount, i.e. fitness). In general the position of i_{th} food source is represented as:

$X_i = (X_{i1}, X_{i2}, \ldots . X_{iD})$.

After the information is shared by the employed bees, onlooker bees go to the region of food source at X_i based on the probability P_i determined as:

$$P_i = \frac{fit_i}{\sum_{k=1}^{FS} fit_k} \quad (22)$$

Where, FS is total number of food sources. Fitness value fit_i is calculated using:

$$fit_i = \frac{1}{1+f(X_i)} \quad (23)$$

Here, $f(X_i)$ is the objective function (J), in this study, an objective function *ITAE* determined from equations (20,21). The onlooker finds its food source in the region of X_i by using the following equation:

$$X_{new} = X_{ij} + r * (X_{ij} - X_{kj}) \quad (24)$$

Where, $k \in (1,2,3,\ldots.FS)$ such that $k \neq i$ and $j \in (1,2,3,\ldots.D)$ are randomly chosen indexes, r is a uniformly distributed random number in the range [-1,1].

If the obtained new fitness value is better than the fitness value achieved so far, then the bee moves to this new food source leaving this old one otherwise it retains its old food source. When all employed bees have completed this process, the information is shared with onlookers. Each of the onlookers selects food source according to probability given above. By this scheme, good sources are well accommodated with onlookers than the bad ones. Each bee will search for a better food source for certain number of cycles (limit), and if fitness value doesn't improve then that particular bee becomes scout bee. In ABC, this is simulated by producing a position of scout bees randomly and replacing it with the abandoned one. Providing that a position cannot be improved further through a predetermined of cycles, then that food source is assumed to be abandoned. The value of predetermined number of cycles is an important control parameter of the ABC algorithm, which is called "limit" for abandonment. Assume that the abandoned source is X_i and $j \in \{1,2,\ldots D\}$, then the scout discovers a new food source to be replaced by X_i. This operation can be expressed in the following relation [37]:

$$X_{new}^{j} = X_{min}^{j} + rand(0,1)(X_{new}^{j} - X_{min}^{j}) \quad (25)$$

3.5 Using ABC-PID controller for estimation of the peak-value for supply reference current

The block diagram for the process of I_{sp}^{*} estimation is demonstrated in figure 4.

The peak value of the supply current can be estimated as follow:

$$I_{sp}^{*} = e(t)K_p + K_i \int_0^{\infty} e(t)dt + K_d \frac{de(t)}{dt} \quad (26)$$

The value of reference current is limited through the range (min. and max.) that are pre-selected values.

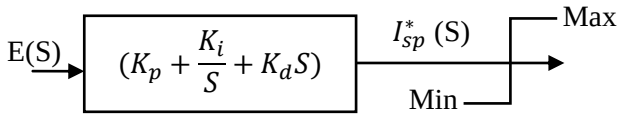

Fig. 4 Estimation of stator ref. current peak value

4 Simulation results and discussion

The proposed system is simulated using the MATLAB/SIMULINK Software [41]. Parameters for supply voltage, transmission line, and un-controlled bridge rectifier, GTO-thyristor dc chopper with snubber circuit, dc motor, SAPF, hysteresis controller, and optimized ABC-PID controller-gains are tabulated in appendix.

The motor uses closed-loop PI-speed controller and results are obtained through starting and steady state running. The results include armature current, torque, and rated speed of the motor. The motor operates at constant full-load torque and speed.

Also, to demonstrate the effect of SAPF on supply currents, it will plot all currents (supply, filter and load currents).

A computer program was written in MATLAB (m-file) to implement the proposed controller design based on bees colony concept. K_p, K_i, K_d, can be defined as:

$$\theta(FS, D) = \begin{vmatrix} K_p^1 & K_i^1 & K_d^1 \\ K_p^2 & K_i^2 & K_d^2 \\ \cdot\cdot & \cdot\cdot & \cdot\cdot \\ K_p^S & K_i^S & K_d^S \end{vmatrix}$$

Where FS= no of food sources, and D is the parameter optimized. In this work, D=3, S=10, and the controller parameters are bounded as:

$\{0, K_{pmax}\}$, $\{0, K_{imax}\}$, $\{0, K_{dmax}\}$

Where,

$0 < K_p \leq 30;\ 0 < K_i \leq 70;\ 0 \leq K_d \leq 0.1$

The peak value of 3-phase supply voltage is 140V as shown in figure 5. Also, the reference dc-link voltage is selected as 250V as shown in figure 6.

Also, the phase shift between supply phase current and voltage- before using SAPF - is shown in figure 7. This angle is approximately equal to 45 degree. Dependently, the supply power factor is ≈ 0.707.

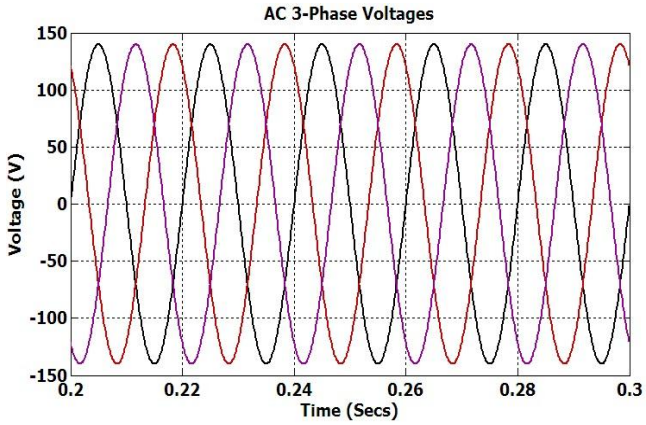

Fig. 5 three-phase ac supply voltages

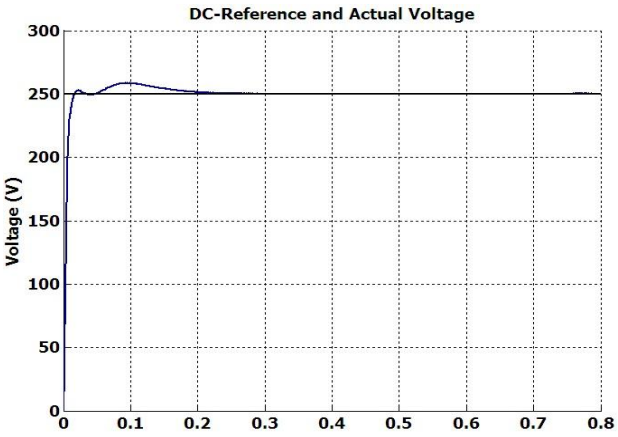

Fig. 6 dc-link actual and reference voltages

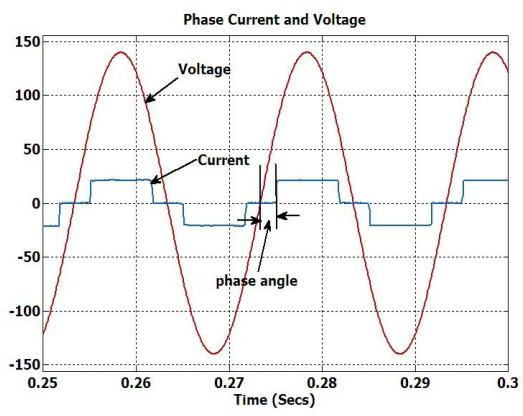

Fig. 7 Phase-shift between supply current and voltage

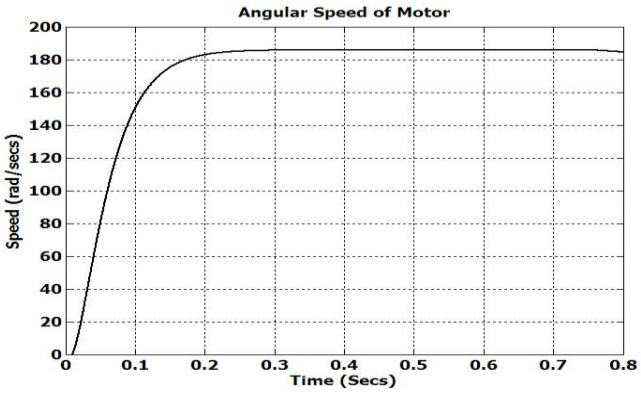

(a) Motor speed

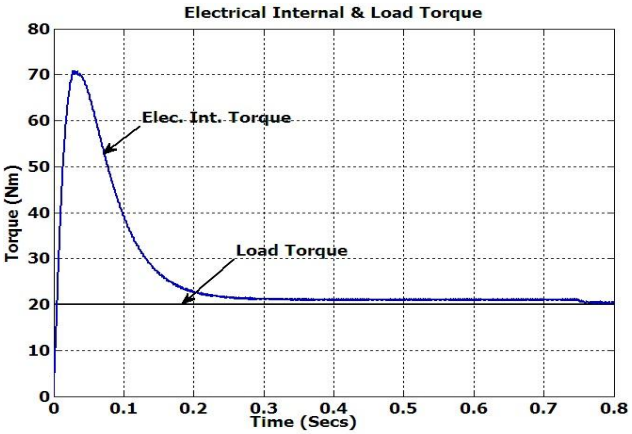

(b) Motor-armature Current

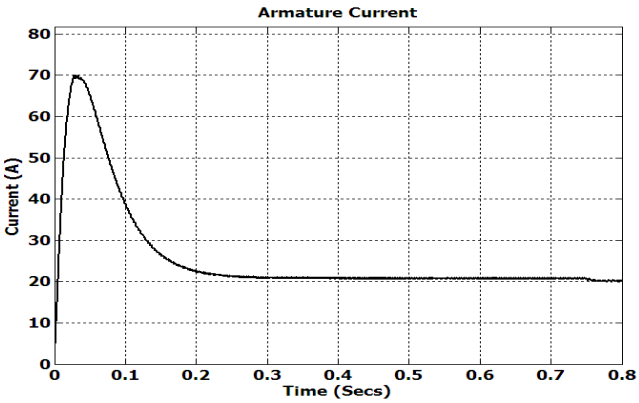

(c) Motor and load torque

Fig. 8 motor speed, current and torque

Figure 6 illustrates the actual and reference dc-link capacitor voltages. Figure 7 shows a bad power factor (p.f) of the supply without SAPF.

Figure (8.a,b,c) shows the motor angular rated speed, armature current, and electrical internal and load torque. The motor armature current is limited to 70A. This leads to increase current above rated value due to starting and the controller can be limit this current and torque but the speed-time response will be affected.

Figure 9 (a,b) clearly illustrates the spectrum fast Fourier transformation (FFT) analysis for the load current and total harmonic distortion (THD) when feeds after SAPF.

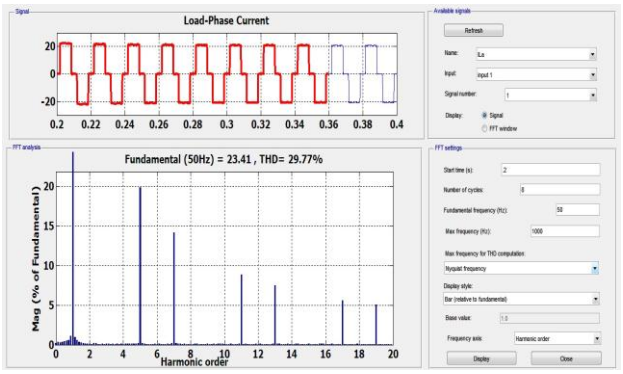

(a) duration time (0.2-0.4)

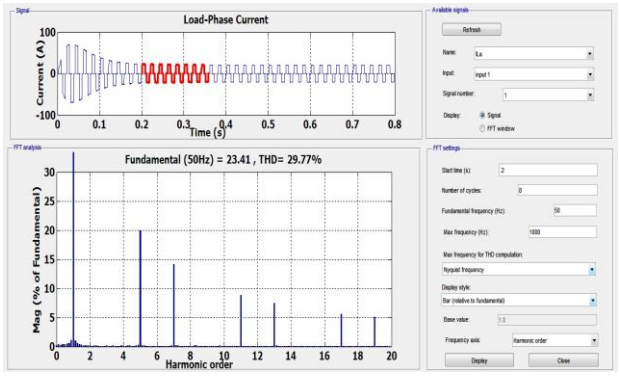

(b) duration time (0.0 – 0.8)

Fig. 9 FFT and THD for load phase current (i_{la})

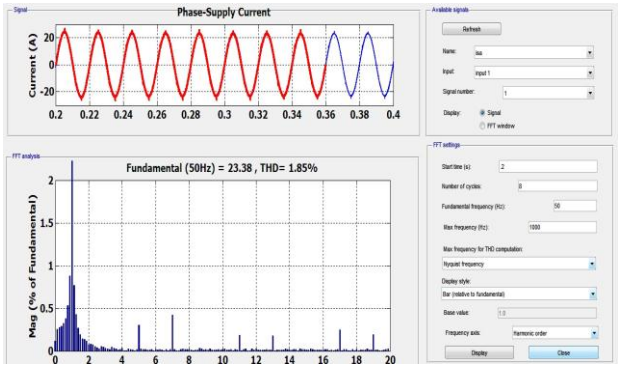

(a) duration time (0.2-0.4)

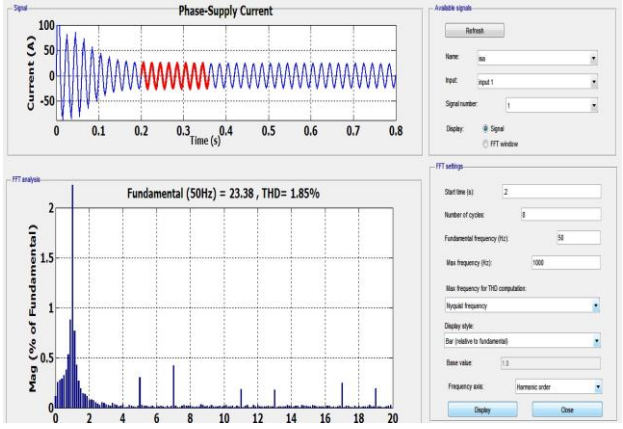

(b) duration time (0.0 – 0.8)

Fig. 10 FFT and THD for supply phase current (i_{sa})

Figure 10 (a,b) clearly illustrates the effect of using SAPF on the supply current. It is turned into approximately pure sinusoidal. Also, the THD is minimized to less than 2% relative to fundamental.

To deduce the effect of the SAPF on the supply power factor (pf), figure 11 shows the phase shift between supply phase-voltage and current. As shown, both waveforms are in phase (zero angle phase shift). This means that the pf of the supply became approximately unity.

Besides, the THD is minimized when using SAPF. As shown in figure 12, the THD for the load is about 30 % and for the supply current is reduced to less than 2%.

Also, the phase current of filter is recorded and plotted as in figure 13 (a,b). This current is a difference between supply and load phase currents that can be determined from equation 2.

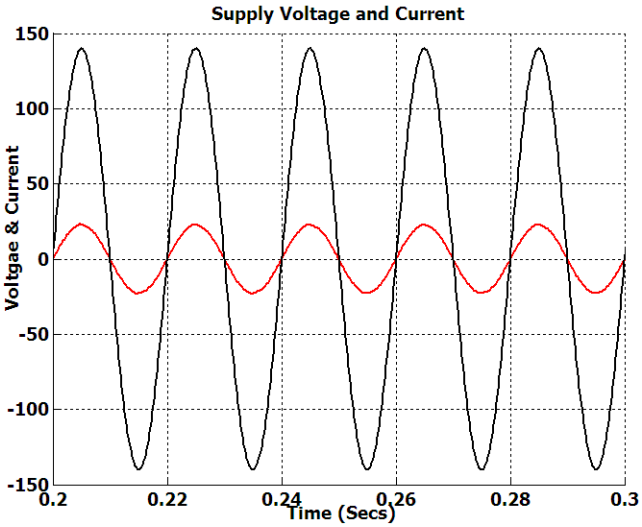

Fig. 11 Supply phase- voltage and current with SAPF

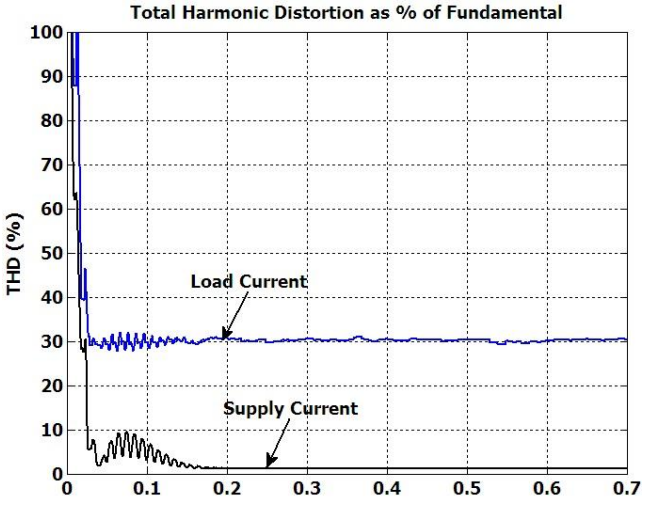

Fig. 12 THD for both load and supply currents with SAPF

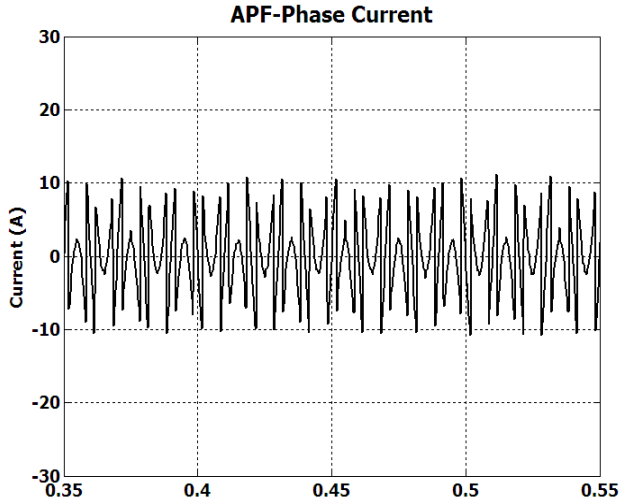

(a) time profile (0.35 – 0.55)

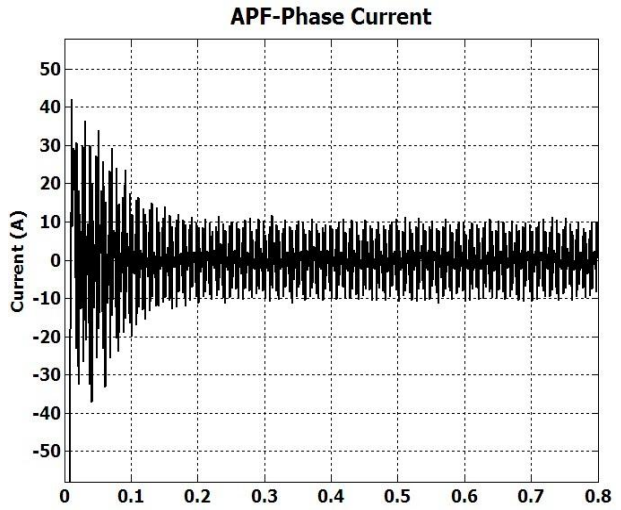

(b) Time profile (0.0-0.8)

Fig. 13 The phase-current of SAPF (i_{fa})

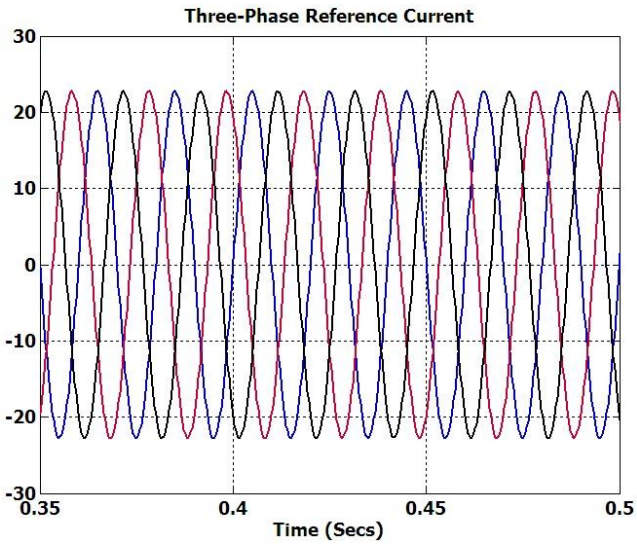

Fig. 14 Three-phase reference currents ($i_{sa}^*, i_{sb}^*, i_{sc}^*$)

Also, the estimated reference supply-phase currents are plotted against time as shown in figure 14.

However, when using SAPF, the supply phase current waveforms and the total harmonic distortion (THD) are enhanced. Also, the supply power factor is improved and increased to unity.

Also, a comparison study will also be done among other intelligent controllers such as artificial neural network (ANN), and fuzzy logic (FL)-PI tuning controllers. Also, the comparison will include classical PID-controller designed by using Ziegler-Nichols formula. The used ANN controller is a feed-forward beck-propagation technique with one input layer, one hidden layer with five neurons, and one output layer [42]. On the other hand, the fuzzy logic self-tuning PI controller is designed as the same technique used in [17].

The classical PID-controller designed by using Ziegler-Nichols formula has the following gains:

$$K_p = 3.1, K_i = 13.22, K_d = .02$$

The following table illustrates the performance of the proposed technique based on the THD. It's observed from the table that the proposed ABC-PID dc-link voltage regulator provides significant performance with 1.85% rather than other techniques.

Table 1: THD comparison

No.	Approach	THD (%)
1	ANN	2.06
2	Fuzzy-PI	2.24
3	Classical PID	3.44
4	ABC-PID	1.85

5. Conclusion

This paper proposes a new optimal control algorithm known as ABC that used in designing of self-tuning self-adaptive PID controller to regulate dc-link capacitor voltage of SAPF. The combination of ABC-controller and the SAPF of the proposed technique is called ABC-SAPF. The proposed ABC-SAPF is used to mitigate line current harmonics and compensate reactive power of the supply feeding a non-linear highly inductive load (DC separately excited dc motor) via a dc chopper and uncontrolled diode-bridge rectifier. The parameters of PID-controller are optimized by using ABC algorithm to give a better performance for the SAPF. The proposed technique is simulated using MATLAB software. Simulation results of dynamic performance for both SAPF and the motor through starting, transient and steady-state conditions, assure the proposed controller in minimizing THD to its minimum value. Also, most

of harmonics are mitigated and the supply power factor (p.f.) is increased to approximately unity. In addition, the performance of that proposed approach is compared with other control strategies such as classical PID, fuzzy-PI, and ANN controllers. However, these results validate the superiority of the proposed method in tuning process compared with other mentioned controllers.

References:

[1] C. Broche et al, Harmonic Reduction in DC by Active Filtering, *IEEE Transactions on Power Electronics*, Vol. 7, NO. 4, Oct. 1992, pp. 633-643.

[2] J. Talla and V. Blahník, Single-Phase Filtering System for DC Motor Locomotives, *International Conference on Clean electrical Power (ICCEP)*, 2013, pp. 712-716.

[3] S. Bhattacharya et al., Flux Based Active Filter Controller, *IEEE Transactions on Industry Applications*, Volume 32, Issue 3, 1996, pp. 491-502.

[4] Hirofumi Akagi, New Trends in Active Filters for Improving Power Quality, *1996., Proceedings of the 1996 International Conference on Power Electronics, Drives and Energy Systems for Industrial Growth*, 1996, vol. 1, pp. 417-425.

[5] B.Singh,K. Al-Haddad and A.Chandra, A New Control Approach to Three-phase Active Filter for Harmonics and Reactive Power Compensation, *IEEE Transactions on Power Systems*, Vol. 13, No. 1, February 1998, pp. 133-138.

[6] IEEE Recommended Practice and Requirements for Harmonic Control in Electric Power Systems, *IEEE Std 519-2014* (Revision of IEEE Std 519-1992), 2014, pp. 1-29.

[7] Electromagnetic compatibility (EMC). Limits. Limits for harmonic current emissions (equipment input current ≤ 16 A per phase), BS EN 61000-3-2, Sept.2014.

[8] H. Akagi et al, A Shunt Active Filter Based on Voltage Detection for Harmonic Termination of a Radial Power Distribution Line, *IEEE Transactions on Industry Applications*, Volume 35, Issue 3, 1999, pp. 638-645.

[9] H. Akagi, Active and Hybrid Filters for Power Conditioning, *Proceedings of the 2000 IEEE International Symposium on Industrial Electronics*, 2000. ISIE 2000.4-8 Dec. 2000, Cholula, Puebla, Mexico, pp. 26-36, vol. 1.

[10] M. Montero, E. Cadaval and F. González, Comparison of Control Strategies for Shunt Active Power Filters in Three-Phase Four-Wire Systems , *IEEE Transactions on Power Electronics*, Vol. 22, No. 1, Jan. 2007, pp 229-236.

[11] D Kucherenko and P Safronov, A Comparison of Time Domain Harmonic Detection Methods for Compensating Currents of Shunt Active Power Filter, *2014 IEEE International Conference on Intelligent Energy and Power Systems (IEPS)*, 2-6 June 2014, Kyiv, Ukraine, pp. 40-45.

[12] S. Biricik et al, Real-Time Control of Shunt Active Power Filter under Distorted Grid Voltage and Unbalanced Load Condition using Self-Tuning Filter, *IET Power Electron.*, 2014, Vol. 7, Issue 7, pp. 1895–1905.

[13] A.Terciyanli et al, A Current Source Converter - Based Active Power Filter for Mitigation of Harmonics at the Interface of Distribution and Transmission Systems, *IEEE Transactions on Industry Applications*, Volume 48, Issue 4, 2012, pp. 1374-1386

[14] Q.Trinh and H. Lee, An Advanced Current Control Strategy for Three-Phase Shunt Active Power Filters, *IEEE Transactions on Industrial Electronics*, Vol. 60, NO. 12, Dec.2013, pp. 5400-5410.

[15] M. Sindhu, M. Nair and T. Nambiar, Dynamic Power Quality Compensator with an Adaptive Shunt Hybrid Filter, *Int. Journal of Power Electronics and Drive System (IJPEDS)*, Vol. 4, No. 4, Dec. 214, pp 508-516.

[16] M. Qasim, P. Kanjiya, and V. Khadkikar, Artificial-Neural-Network-Based Phase-Locking Scheme for Active Power Filters, *IEEE Transactions on Industrial Electronics*, Vol. 61, No. 8, Aug. 2014, pp. 3857-3866.

[17] Y. Suresh A.K. Panda M. Suresh, Real-Time Implementation of Adaptive Fuzzy Hysteresis-Band Current Control technique for Shunt Active Power Filter, *IET Power Electron.*, Vol. 5, Issue 7, 2012, pp. 1188–1195.

[18] N. Eskandarian, Y. Beromi, and S. Farhangi , Improvement of Dynamic Behavior of Shunt Active Power Filter Using Fuzzy Instantaneous Power Theory, *Journal of Power Electronics*, Vol. 14, No. 6, pp. 1303-1313, November 2014, pp. 1303-1312.

[19] L. Saribulut1, A.Teke, and M. Tüma, Artificial Neural Network-Based Discrete-Fuzzy Logic Controlled Active Power Filter, *IET Power Electronics*, 2014, Vol. 7, Issue 6, pp. 1536–1546.

[20] S.Suresh and S.Kannan, DC Link Voltage Regulated Active Power Line Conditioner for Compensating Harmonic and Reactive Power, *2011 International Conference on Recent Advancements in Electrical, Electronics and*

Control Engineering, 15-17 Sep. 2011, College Sivakasi , India, pp. 87-90.

[21] S. Rahmani et al, A Combination of Shunt Hybrid Power Filter and Thyristor-Controlled Reactor for Power Quality, *IEEE Transactions on Industrial Electronics*, Vol. 61, No. 5, May. 2014, pp. 2152-2164.

[22] S. Biricik et al, Real-Time Control of Shunt Active Power Filter Under Distorted Grid Voltage and Unbalanced Load Condition using Self-Tuning Filter, *IET Power Electronics*, 2014, Vol. 7, Issue 7, pp. 1895–1905.

[23] R.Ribeiro, C. Azevedo, and R. M. Sousa, A Robust Adaptive Control Strategy of Active Power Filters for Power-Factor Correction, Harmonic Compensation, and Balancing of Non -linear Loads, *IEEE Transactions on Power Electronics*, Vol. 27, NO. 2, Feb. 2012, pp. 718-730.

[24] R.Ribeiro, T. Rocha, and R. M. Sousa, A Robust DC-Link Voltage Control Strategy to Enhance the Performance of Shunt Active Power Filters without Harmonic Detection Schemes, *IEEE Transactions on Industrial Electronics*, 2013, Citation information: DOI 10.1109 / TIE. 2014. 2345329.

[25] B. Angélico, L. Campanhol, and S. Silva, Proportional – Integral / Proportional–Integral Derivative Tuning Procedure of a Single-Phase Shunt Active Power Filter Using Bode Diagram, *IET Power Electronics*, 2014, Vol. 7, Issue 10, pp. 2647–2659.

[26] Sreeraj E. S. et al, An Active Harmonic Filter Based on One-Cycle Control, *IEEE Transactions on Industrial Electronics*, Vol. 61, No. 8, Aug. 2014, pp. 3709-3809.

[27] L. Yang, A Stable Self-Learning PID Control Based on the Artificial Immune Algorithm, *Proc. of the IEEE Inter. Conf. on Automation and Logistics*, Shenyang, China, Aug. 2008, pp. 1237-1242.

[28] Q. Zeng and G. Tan, Optimal Design of PID Controller using Modified Ant Colony System Algorithm", *IEEE Third Int. Conf. on Natural Computation (ICNC'07)*, 24-27Aug. 2007, China

[29] H. I. Abdul-ghaffar Essamudin. A. E. and M. Azzam, Design of PID Controller for Power System Stabilization Using Hybrid Particle Swarm-Bacteria Foraging Optimization, *WSEAS Transaction on Power Systems*, Issue 1, Volume 8, January 2013, pp. 12-23.

[30] A. S. Oshaba and E. S. Ali, Bacteria Foraging: A New Technique for Speed Control of DC Series Motor Supplied by Photovoltaic System, *WSEAS Transaction on Power Systems*, Volume 9, 2014, pp. 185-195.

[31] P. Saravanan and P. Balakrishnan, An Efficient BFO Algorithm for Self Tuning Pi-Controller Parameters for Shunt Active Power Filter, *WSEAS Transaction on Power Systems, Volume 9*, 2014, pp. 155-170.

[32] Darvis. Karaboga, An Idea Based on Honey Bee Swarm for Numerical Optimization Technique, *Report-06*, Erciyes University Engineering Faculty, Computer Engineering Department 2005.

[33] B. Basturk, D. Karaboga, An Artificial Bee Colony (ABC) Algorithm for Numeric Function Optimization, *IEEE Swarm Intelligence Symposium 2006*, Indianapolis, Indiana, USA,2006.

[34] N. Elkhateeb and R. Badr, Employing Artificial Bee Colony with Dynamic Inertia Weight for Optimal Tuning of PID Controller, *U2013 Proceedings of Int. Conf. On Modelling, Identification & control (ICMIC)*, Cairo, Egypt, 31th Aug. – 2nd Sep. 2013, pp. 42-46.

[35] A. Rahim, M. Ali, Tuning of PID SSSC Controller Using Artificial Bee Colony Optimization Technique, *2014 11th International Multi-Conference on Systems, Signals & Devices* , 11-14 Feb 2014, Barcelona, Spain, pp. 1-6.

[36] W. Liao, Y. Hu, and H. Wang, Optimization of PID Control for DC Motor Based on Artificial Bee Colony Optimization, *Proceedings of the 2014 Int. Conf. on Advanced Mechatronics Systems*, Kumamoto , Japan, 10-12 Aug., 2014, pp. 23-27.

[37] Essamudin A. E., "Artificial Bee Colony-Based Design of Optimal On-Line Self-tuning PID-Controller Fed AC Drives", *International Journal of Engineering Research (IJER)*, Vol. No.3, Issue No.12, 1 Dec. 2014, pp. 807-811.

[38] P. Pejovic, *Three-Phase Diode Rectifiers with Low Harmonics*, Book chapter 2, Springer Publishing, 2007.

[39] J. Arrillaga and N. R. Watson, *Power System Harmonics*, 2nd Edition, John Wiley & sons, USA , 2004.

[40] Bill Drury, *The Control Technique Drives and Controls*, Handbook, IEE Power and Energy Series 35, The Institute of Electrical Engineers, London, UK, 2001.

[41] Mathwork Co., "*MATLAB Software Manual*", USA 2014.

[42] Essamudin A. E., *Artificial Neural Network-Based Tracking Adaptive Vector-Control of Three-Phase Induction-Motor Servo-Drives*, Ph.D. thesis, Cairo University, 2001.

[43] G. El-Saady, A. El-Sayed, Essamudin A. E., and H. I. Abdul-Ghaffar, Harmonic Compensation Using On-Line Bacterial Foraging Optimization Based Three-Phase Active Power Filter, *WSEAS*

Transaction on Power Systems, Volume 10, 2015, pp. 73-81.

[44] Essamudin A. E., A Novel Approach of Bacteria-Foraging Optimized Controller for DC Motor and Centrifugal Pump Set Fed from Photo-Voltaic Array, *Journal of Next Generation Information Technology (JNIT)*, Volume 6, Number 1, February 2015, pp. 21-31.

[45] H. I. Abdul-ghaffar Essamudin. A. E. and M. Azzam, Design of PID Controller for Power System Stabilization Using Ant Colony Optimization Technique, *Middle East Power Conference (MEPCON'14)*, Cairo 2014, EGYPT.

[46] Essamudin A. E., G. El-saady, Y. S. Mohamed, H. I. Abdul-Ghaffar, Particle Swarm Optimization- Based Control of Three-Phase Active-Power Filter for Harmonic Mitigation, *Industrial and Academia Collaboration Conference*, Cairo 6-8 April 2015.

[47] S. Staines A., and Neri F., A Matrix Transition Oriented Net for Modelling Distributed Complex Computer and Communication Systems, *WSEAS Transactions on Systems*, 13, WSEAS Press (Athens, Greece), 2014, pp.12-22.

[48] Camilleri M., Neri F., and Papoutsidakis M., An Algorithmic Approach to Parameter Selection in Machine Learning using Meta-Optimization Techniques, *WSEAS Transactions on Systems*, 13, WSEAS Press (Athens, Greece), 2014, pp. 202-213.

[49] M Papoutsidakis, D Piromalis, F Neri, and M Camilleri, Intelligent Algorithms Based on Data Processing for Modular Robotic Vehicles Control, *WSEAS Transactions on Systems*, 13, WSEAS Press (Athens, Greece), 242-251.

Appendix:

DC motor parameters	value
Rated Voltage	240V
Rated Power	5HP
Rated Armature Current	5.5 Amps
Rated Speed	1750 rpm
Rated field voltage	300V
Armature Resistance and Inductance	2.581 Ω , 0.028H
Field Resistance and Inductance	281.3 Ω, 156 H
Field-Armature Mutual Inductance	0.94483 H
Total Rotor Inertia	.02215 Kg.m²
Viscous Friction Coefficient	0.002953 Nms
Columb Friction Torque	0.5161 Nm

	Nonlinear system parameters	Value
1	Supply phase peak voltage, V_m	140 V
2	Supply rated frequency, f	50 Hz
3	Supply resistance, R_s	0.1Ω,
4	Supply inductance, L_s	0.15mh
5	Filter resistance, R_f	0.1Ω,
6	Filter inductance, L_f	0.335mH
7	DC Capacitance, C_d	2000 µF
8	DC reference voltage, V_{dc}	250 V
9	Hysteresis band current (HB)	0.1A

ABC-algorithm parameters	value
Number of Colony Size=Np	20
Number of Food Sources (S=Np/2)	10
Maximum Number of Cycles	50
Threshold Probability	0.75
Number of Optimized Parameters	3